Available online at www.sciencedirect.com

ScienceDirect

www.elsevier.com/locate/jes

JES JOURNAL OF ENVIRONMENTAL SCIENCES

www.jesc.ac.cn

Acute and chronic toxicity of nickel to nitrifiers at different temperatures

Xiaoguang Liu[1], *Mohammad M.I. Chowdhury*[1], *Masuduz Zaman*[2], *Mingu Kim*[2], *George Nakhla*[1,2,*]

1. *Department of Civil and Environmental Engineering, University of Western Ontario, London, Ontario N6A 5B9, Canada*
2. *Department of Chemical and Biochemical Engineering, University of Western Ontario, London, Ontario N6A 5B9, Canada*

ARTICLE INFO

Article history:
Received 7 February 2019
Revised 13 March 2019
Accepted 13 March 2019
Available online 21 March 2019

Keywords:
Nickel inhibition
Temperature
Nitrifying culture
Activated sludge
Toxicity

ABSTRACT

This study investigated the acute nickel toxicity on nitrification of low ammonia synthetic wastewater at 10, 23, and 35°C. The nickel inhibition half-velocity constants ($K_{I,Ni}$) for ammonia oxidizing bacteria (AOB) and nitrite oxidizing bacteria (NOB) based on Ni/MLSS ratio at 10, 23, and 35°C were 5.4 and 5.6 mg Ni/g MLSS, 4.6 and 3.5 mg Ni/g MLSS, and 9.1 and 2.7 mg Ni/g MLSS, respectively. In addition, chronic toxicity of nickel to nitrification of low ammonia synthetic wastewater was investigated at 10°C in two sequencing batch reactors (SBRs). Long-term SBRs operation and short-term batch tests were comparable with respect to the extent of inhibition and corresponding Ni/MLSS ratio. The μ_{max}, b, and K_o of AOB were 0.16 day^{-1}, 0.098 day^{-1} and 2.08 mg O_2/L after long-term acclimatization to nickel of 1 mg/L at 10°C, high dissolved oxygen (DO) (7 mg/L) and long solids retention time (SRT) of 63–70 days. Acute nickel toxicity of nitrifying bacteria was completely reversible.

Introduction

Nitrification is a two-step process involving nitritation (ammonia oxidation to nitrite) by ammonia oxidizing bacteria (AOB) and nitratation (nitrite oxidation to nitrate) by nitrite oxidizing bacteria (NOB) (Metcalf and Eddy, 2013). Both AOB and NOB are autotrophs (Metcalf and Eddy, 2013). Nitrifiers are affected by environmental conditions such as pH, dissolved oxygen (DO) concentrations, temperature, and toxic chemicals (Aslan and Sozudogru, 2017; Ge et al., 2015; Soliman and Eldyasti, 2018).

A variety of organic and inorganic chemical species can affect the specific growth rate of the nitrifiers (Blum and Speece, 1991). Heavy metals pose acute and sub-chronic toxicological effects on the ecosystem (Akhtar et al., 2018). The influence of heavy metals on the conventional activated sludge system has been thoroughly studied (Cheng et al., 2011; Dilek and Gökçay, 1996; Hernandez-Martinez et al., 2018; Stasinakis et al., 2002; Sun et al., 2017; Yang et al., 2017; Yuan et al., 2014). The influence of heavy metals on nitrifying bacteria is of interest because these metals and their complexes can potentially inhibit nitrification by disrupting proteins after transport across bacterial cell membranes and interacting with protein functional groups (Gadd and Griffiths, 1977; Kapoor et al., 2015; Nies, 1999; Yin et al., 2016).

Nickel (Ni) is a common metal which exists at various ranges in the influents of different wastewater treatment plants. Although the typical influent nickel concentration in municipal wastewater treatment plant (MWWTP) is low (<50 μg/L) (Chipasa, 2003; Carletti et al., 2008), still some plants receiving industrial wastes may suffer from high

* *Corresponding author at: E-mails:* xliu625@uwo.ca, (Xiaoguang Liu), gnakhla@uwo.ca. (George Nakhla).

https://doi.org/10.1016/j.jes.2019.03.009
1001-0742 © 2019 The Research Center for Eco-Environmental Sciences, Chinese Academy of Sciences. Published by Elsevier B.V.

influent nickel concentrations, as shown by the following cases. Carletti et al. (2008) reported an influent nickel concentration of 3.5–61.7 μg/L from 5 MWWTPs in Italy. A higher influent nickel concentration range of 20.2–107.6 μg/L from the Depurbaix (Barcelona, Spain) MWWTP was reported by Teijon et al. (2010). The report of European Communities: *Pollutants in urban wastewater and sewage sludge* reported that nickel concentration in municipal wastewater ranged from 40 to 170 μg/L in Austria (Communities, 2001). A high influent nickel concentration of up to 970 μg/L in Thessaloniki (Greece) MWWTP was reported by Karvelas et al. (2003).

The three most important factors of nickel inhibition on nitrification are: (1) the sludge type i.e., either activated sludge or nitrifying culture; (2) the exposure mode, either long-term dose or short-term; and (3) the temperature (Gikas, 2008; Li et al., 2016). Although very limited studies compared the acute and chronic nickel toxicity to nitrification, the effect of acute and chronic nickel toxicity to various microorganisms have been reported and compared (Keithly et al., 2004; Leonard et al., 2011). Studies on nickel inhibition of nitrification are summarized in Appendix A Table SI 1. Due to differences in sludge type, exposure mode, and temperature, the literature results are not always consistent (Aslan and Sozudogru, 2017; Hu et al., 2004; Randall and Buth, 1984; Yeung et al., 2013; You et al., 2009). There is no clear conclusion and it is hard to tell which one is the most important among the three factors, sludge type, exposure time or temperature. Pereira et al. (2017) studied the effect of temperature on chronic copper, zinc, and nickel toxicity to *D. magna* at 15, 20, and 25°C and reported that chronic Cu, Zn, and Ni toxicity to *D. magna* were all significantly affected by temperature. In addition, Buch et al. (2016) studied acute and chronic ecotoxicity of mercury to *Folsomia candida* and *Proisotoma minuta*, and reported different EC50 for the two species at 20 and 24°C. From Appendix A Table S1, the effect of temperature on nickel toxicity to nitrifying bacteria was not studied comprehensively and systematically. Only one study by Randall and Buth (1984) reported the chronic nickel effect on nitrification of activated sludge at 14, 17, and 35°C. In addition, most of the studies focused on nickel toxicity of AOB while limited information about nickel toxicity of NOB has been reported (Aslan and Sozudogru, 2017; Çeçen et al., 2010; Hu et al., 2003; Insel et al., 2006; Kapoor et al., 2015). Furthermore, in the previous short-term batch tests, the effect of biomass concentration was neglected as nickel concentration was chosen as the only variable with constant biomass and temperature (Hu et al., 2003; Hu et al., 2004; Kapoor et al., 2015; You et al., 2009). However, in this study we varied both the nickel and biomass concentrations in the batch tests to assess whether the parameter affecting nickel inhibition is the absolute nickel concentration or the nickel-to-biomass ratio. Lastly, to date, the long-term effect of nickel on nitrification performance of nitrifying cultures at temperatures as low as 10°C has not been studied.

In this study, we compared different sludge type, i.e., nitrifying culture and return activated sludge (RAS), different exposure mode, i.e., chronic versus acute, and different temperatures. Thus, this study investigated the nickel toxicity to nitrifiers comprehensively and systematically. This study aims to assess: (1) which factor is the most important i.e., sludge type, exposure time, or temperature; (2) how nickel toxicity of AOB and NOB differ at different temperatures; (3) how chronic and acute nickel toxicity differ from each other; (4) how long-term acclimatization affects the nickel toxicity. In addition, the reversibility of acute nickel toxicity to nitrification was tested.

1. Methodology

1.1. Nitrification reactors

Two SBRs with a working volume of 10 L were used in this study. For each SBR, two pumps (Masterflex L/S, Cole-Parmer, Montreal, Canada) were used, one feeding the wastewater to the SBR and the other withdrawing the effluent. Aeration was provided with an air pump (Rena Air 400, Rena Aquatic Supply, Charlotte, USA) through an air diffuser. The SBRs were operated at 10°C with a water bath (PolySciences Heated Circulating Bath, 1 SD07R-20-A11B). The SBRs were aerated to affect a DO of 7 mg/L during mixing. Each cycle consisted of 20 min feed, 650 min aerobic reaction, 30 min settling, and 20 min effluent discharge. In each cycle, 5 L of supernatant were withdrawn from the SBRs after the settling phase, and replaced with fresh wastewater, resulting in an exchange ratio of 50%. pH was not controlled, and during each cycle pH decreased with time. No sludge discharge was carried out and the SRTs were estimated based on reactor and effluent biomass.

The operation of SBR 1 can be divided into two phases, that is, phase 1 from day 0 to day 94 with no nickel addition, and phase 2 from day 95 to day 137 with 1.0 mg/L of nickel addition. SBR2 was operated with a nickel dose of 1.0 mg/L from the beginning to the end. 1.0 mg/L of nickel dose was used as practically it is reported upper concentration limit in municipal wastewater (Karvelas et al., 2003). In addition, 1.0 mg/L has been reported as an important cutoff inhibition level in some studies (Aslan and Sozudogru, 2017; Yeung et al., 2013).

1.2. Synthetic wastewater and activated sludge characteristics

The synthetic wastewater was composed of NH_4Cl (40–60 mg N/L), $NaHCO_3$ (480–720 mg/L), KH_2PO_4 (8–12 mg P/L), $MgSO_4{\cdot}7H_2O$ (100 mg/L), $CaCl_2$ (100 mg/L), 1 mL/L water of trace elements solution I (composition in g/L as follows: EDTA 15, $ZnSO_4$ 0.43, $CoCl_2$ 0.24, $MnCl_2$ 0.63, $CuSO_4$ 0.25, Na_2MoO_4 0.22, $NiCl_2$ 0.19, Na_2SeO_4 0.21, H_3BO_3 0.01, and $NaWO_4$ 0.05), and 1 mL/L water of trace elements solution II containing $FeSO_4$ and EDTA at 5 g/L each (Liu et al., 2017a). The alkalinity to ammonia-nitrogen ratio was 7.17:1 (Metcalf and Eddy, 2013). RAS from the Greenway wastewater treatment plant in London, Ontario was used as the inoculum to start the SBRs.

1.3. Analytical methods

Effluent ammonia, nitrite, and nitrate were measured using HACH methods (10,031, 8153/10,019 and 8039) every two days (Liu et al., 2017a, 2018). Mixed liquid suspended solids (MLSS) concentrations in the SBR and SBR effluents were measured

in triplicates using Whatman GF/A filters (VWR International, Mississauga, Canada), in accordance with Standard Methods (APHA, 2005) once a week. Nickel concentrations in the influent, SBR, and effluent were measured by inductively coupled plasma optical emission spectrometry (ICP-OES) (Vista-Pro, VARIAN) with a flame temperature in a range from 6000 to 10,000K according to Standard Methods (3120) (APHA, 2005) after acid digestion with HNO_3 and filtration through a 0.45 μm filter paper. The pH of the filtrate was adjusted to below 2, using concentrated nitric acid (67%–70%) prior to measurement. The detection limit of nickel was 0.01 mg/L.

Dissolved oxygen and pH were measured using a dissolved oxygen meter (HACH HQ 40d) and a pH meter (VWR B10P), respectively.

1.4. Online batch tests

Online batch tests were conducted in SBR 2 between days 120 and 140 at three different DO levels (3.0, 5.0, and 7.4 mg/L, respectively) with a dose of 1.0 mg/L of nickel to determine the biomass ammonia oxidation rate (AOR) and nitrite oxidization rate (NOR) (Liu and Wang, 2014; Liu et al., 2017a).

At the end of the study, the reactor was fed with deionized water and 1 mg/L of nickel, mixed, and aerated for 12 days to determine the decay coefficient (b) (Liu et al., 2017a). The biomass concentration was measured every two to three days.

Kinetic modeling was carried out based on the important pertinent equations summarized below (Liu et al., 2018):

$$Y \times Q \times (S_0 - S) - b \times V \times X - \frac{VX}{SRT} = 0 \quad (1)$$

Where Y (mg VSS/mg N) is yield coefficient; Q (L/day) is flow rate; S_0 (mg N/L) and S (mg N/L) are influent and effluent substrate concentration; b (day^{-1}) is decay coefficient, V (L) is reactor volume; X (mg VSS/L) is biomass concentration; SRT (day) is solids retention time.

$$X_{AOB} = \frac{Y_{AOB} \times Q \times (S_{0,NH} - S_{NH})}{V \times \left(b + \frac{1}{SRT}\right)} = \frac{SRT}{HRT} \frac{Y_{AOB} \times (S_{0,NH} - S_{NH})}{1 + b \times SRT} \quad (2)$$

$$X_{NOB} = \frac{Y_{NOB} \times Q \times (S_{NO3} - S_{0,NO3})}{V \times \left(b + \frac{1}{SRT}\right)} = \frac{SRT}{HRT} \frac{Y_{NOB} \times (S_{NO3} - S_{0,NO3})}{1 + b \times SRT} \quad (3)$$

$$q = \frac{\mu}{Y} \quad (4)$$

$$AOR = X_{AOB}\ q_{AOB} = q_{AOB} \times \frac{SRT}{HRT} \frac{Y_{AOB} \times S_{0,NH} - S_{NH}}{1 + b \times SRT} \quad (5)$$

$$NOR = X_{AOB}\ q_{AOB} = q_{NOB} \times \frac{SRT}{HRT} \frac{Y_{NOB} \times (S_{NO3} - S_{0,NO3})}{1 + b \times SRT} \quad (6)$$

$$\mu_{AOB} = \frac{AOR \times HRT \times \left(b_{AOB} + \frac{1}{SRT}\right)}{S_{0,NH} - S_{NH}} \quad (7)$$

$$\mu_{NOB} = \frac{NOR \times HRT \times \left(b_{AOB} + \frac{1}{SRT}\right)}{S_{NO3} - S_{0,NO3}} \quad (8)$$

where μ_{AOB} (day^{-1}) and μ_{NOB} (day^{-1}) are the biomass-specific growth rates of AOB and NOB, respectively; b_{AOB} (day^{-1}) and b_{NOB} (day^{-1}) are endogenous decay coefficients for AOB and NOB, respectively; Y_{AOB} (mg VSS/mg N) and Y_{NOB} (mg VSS/mg N) are biomass yield coefficients for AOB and NOB, respectively; q_{AOB} (mg N/(mg VSS day)) and q_{NOB} (mg N/(mg VSS day)) are the maximum specific substrate utilization rates for AOB and NOB, respectively; X_{AOB} (mg VSS/L) and X_{NOB} (mg VSS/L) are the active AOB and NOB biomass concentrations, respectively; AOR (mg N/hr) and NOR (mg N/hr) are the ammonia oxidation rate and nitrite oxidation rate, respectively; S_{NH} (mg N/L) and S_{NO3} (mg N/L) are effluent ammonia and nitrate concentrations, respectively; ($S_{0,NH} - S_{0,NH}$) (mg N/L) and ($S_{NO3} - S_{0,NO3}$) (mg N/L) are ammonia and nitrite oxidized, respectively; and HRT (day) is the hydraulic retention time.

In addition, the Monod model was used in this study to calculate AOR_{max} and NOR_{max} as well as the DO-half saturation concentration (K_o), as shown below:

$$AOR = AOR_{max} \times \frac{DO}{DO + K_{o,AOB}} \quad (9)$$

$$NOR = NOR_{max} \times \frac{DO}{DO + K_{o,NOB}} \quad (10)$$

Where AOR_{max} (mg N/hr) and NOR_{max} (mg N/hr) are the maximum ammonia oxidation and nitrite oxidation rates, respectively; DO (mg O_2/L) is dissolved oxygen concentration; $K_{o,AOB}$ (mg O_2/L) and $K_{o,NOB}$ (mg O_2/L) are the AOB and NOB DO-half saturation concentration, respectively.

The ammonia conversion ratio (ACR) and nitrite accumulation ratio (NAR) were calculated based on influent and effluent quality as shown below in Eqs. (11) and (12).

$$ACR = \frac{S_{0,NH} - S_{NH}}{S_{0,NH}} \quad (11)$$

$$NAR = \frac{S_{NO2}}{S_{NO2} + S_{NO3}} \quad (12)$$

Where $S_{0,NH}$ is the influent ammonia concentration, and S_{NH}, S_{NO2}, and S_{NO3} are the effluent concentrations of ammonia, nitrite, and nitrate, respectively.

1.5. Offline batch tests

Acute nickel toxicity to nitrification was determined using offline batch tests in small beakers (500 mL) using RAS from the Greenway wastewater treatment plant. The design of the offline batch tests is depicted in Table 1. The initial ammonia concentration in the batch tests was 25–30 mg N/L with an alkalinity-to-nitrogen ratio of 7.14 mg $CaCO_3$/mg N. A constant DO of 7 mg/L, similar to the ambient DO in the SBR during the aerobic reaction phase, was maintained by monitoring the DO every 15 min and adjusting the airflow rate accordingly from 1.0 to 1.5 L/min. The batch tests were conducted at 10, 23, and 35°C. The experimental time varied from 2 to 24 hr for the different batches based on ammonia conversion rate and nitrite conversion rate. The objective of batches A–E was to evaluate the effect of different nickel concentrations on nitrification with the same MLSS

Table 1 – Offline batch tests design.

	A	B	C	D	E	F	G	H	I
Ni concentration (mg/L)	0	0.5	1.0	1.5	2.0	1.0	1.0	1.0	1.0
MLSS concentration (mg/L)	340	340	340	340	340	680	1020	1360	2720
MLVSS concentration (mg)	260	260	260	260	260	520	780	1040	2080

concentration. The objective of batches C & F-I was to evaluate the effect of same nickel concentration on nitrification at different MLSS concentrations. Samples were taken with time regularly and ammonia, nitrite, and nitrate were determined.

1.6. Short-term nickel inhibition modeling

As nickel is not a substrate for nitrifying bacteria, the inhibition of nickel may potentially be modeled by non-competitive inhibition model, as shown in Eqs. (13)–(16) (Lewandowski, 1987).

$$SAOR = SAOR_{max} \times \frac{K_{I,Ni}}{K_{I,Ni} + Ni} \quad (13)$$

$$SNOR = SNOR_{max} \times \frac{K_{I,Ni}}{K_{I,Ni} + Ni} \quad (14)$$

$$\frac{1}{SAOR} = \frac{Ni}{SAOR_{max} \times K_{I,Ni}} + \frac{1}{SAOR_{max}} \quad (15)$$

$$\frac{1}{SNOR} = \frac{Ni}{SNOR_{max} \times K_{I,Ni}} + \frac{1}{SNOR_{max}} \quad (16)$$

Where SAOR (mg N/g MLSS-hr) and SNOR (mg N/g MLSS-hr) are the biomass-specific ammonia oxidation and nitrite oxidation rates, respectively; $SAOR_{max}$ (mg N/g MLSS-hr) and $SNOR_{max}$ (mg N/g MLSS-hr) are the maximum specific ammonia oxidation and specific nitrite oxidation rates, respectively; $K_{I,Ni}$ (mg Ni/L) is the half-velocity inhibition nickel concentration.

In this study, as the toxicity of nickel is a function of Ni/MLSS ratio (Randall and Buth, 1984; Sujarittanonta and Sherrard, 1981), a modified non-competitive inhibition model based on Ni/MLSS ratio (Eqs. (17)–(20)), was used.

$$SAOR = SAOR_{max} \times \frac{K_{I,Ni/MLSS}}{K_{I,Ni/MLSS} + Ni/MLSS} \quad (17)$$

$$SNOR = SNOR_{max} \times \frac{K_{I,Ni/MLSS}}{K_{I,Ni/MLSS} + Ni/MLSS} \quad (18)$$

$$\frac{1}{SAOR} = \frac{Ni/MLSS}{SAOR_{max} \times K_{I,Ni/MLSS}} + \frac{1}{SAOR_{max}} \quad (19)$$

$$\frac{1}{SNOR} = \frac{Ni/MLSS}{SNOR_{max} \times K_{I,Ni/MLSS}} + \frac{1}{SNOR_{max}} \quad (20)$$

where SAOR, SNOR $SAOR_{max}$, and $SNOR_{max}$ are as described above for Eqs. (13)–(16). $K_{I,Ni/MLSS}$ (mg Ni/g MLSS) is the half-velocity inhibition constant based on Ni/MLSS ratio.

1.7. Acute toxicity reversibility tests

The reversibility of the acute nickel toxicity was investigated through offline batch tests in 500 mL beakers at 23°C using RAS from the Greenway wastewater treatment plant in London, Ontario. Batch tests A, B, and C had the same initial biomass concentration (340 mg MLSS/L). The initial ammonia concentration was around 26 mg N/L with an alkalinity-to-nitrogen ratio of 7.14 mg $CaCO_3$/mg N. In batch test A, nitrification was conducted without nickel. In batch test B, the RAS was first inhibited by nickel dose of 1 mg/L for 2 hr, after which the RAS was washed, resuspended in the same nitrifier medium as test A, and tested for nitrification activity. In batch test C, nitrification was conducted with 1 mg/L of nickel. Samples were taken every two hours and ammonia, nitrite, and nitrate were determined.

1.8. Calculation of nickel speciation

Heavy metals speciation was theoretically calculated using Visual MINTEQ version 3.1 (Gustafsson, 2013). This theoretical speciation was carried out considering the pH, the initial heavy metal concentration used in each batch test, as well as the total anions and cations concentration of the synthetic wastewater. The composition of the influent for nickel speciation calculations are: NH_4Cl 115 mg/L, $NaHCO_3$ 360 mg/L, $NiCl_2$ 2.2 mg/L. The pH of the influent is 7.3 and the calculation was conducted at 10, 23 and 35°C.

1.9. Statistical analysis

One-wayANOVA analysis was conducted using Excel on the effluent quality data of SBR 1 phase 1 (days 0–90) and SBR 2 phase 2 (days 35–96) within which the Ni/MLSS ratio in both SBRs varied from 0 to 2.7 mg Ni/g MLSS, and SBR 1 phase 2 (days 95–137) and SBR 2 phase 4 (days 117–163) within which the Ni/MLSS ratio in both SBRs varied from 4 to 7 mg Ni/g MLSS. The aim of the one-way ANOVA analysis was to judge whether the effluent quality data of the aforementioned phases are the same or different.

2. Results and discussion

2.1. SBR performance

Fig. 1a and b shows the nitrification performance of SBR 1 and SBR 2, respectively, with the summary depicted in Appendix A Table SI 2.

For SBR1, after a quick acclimatization period (<10 days), a relatively stable effluent quality was observed during phase 1. AOBs were not able to convert all the ammonia, due to the low activity of AOB at low temperature (10°C). The average ACR and NAR were 79.1% ± 7.5% and 4.5% ± 1.8%, respectively. At 10°C, the NOB growth rate is higher than that of AOB (Hellinga et al., 1998; Zhu et al., 2008). At high DO (7.0 mg/L), NOB activity was not limited (Liu et al., 2017b). As a result, the rate-limiting step was the ammonia oxidation by the AOB rather than NOB, and full nitrification was achieved. At the

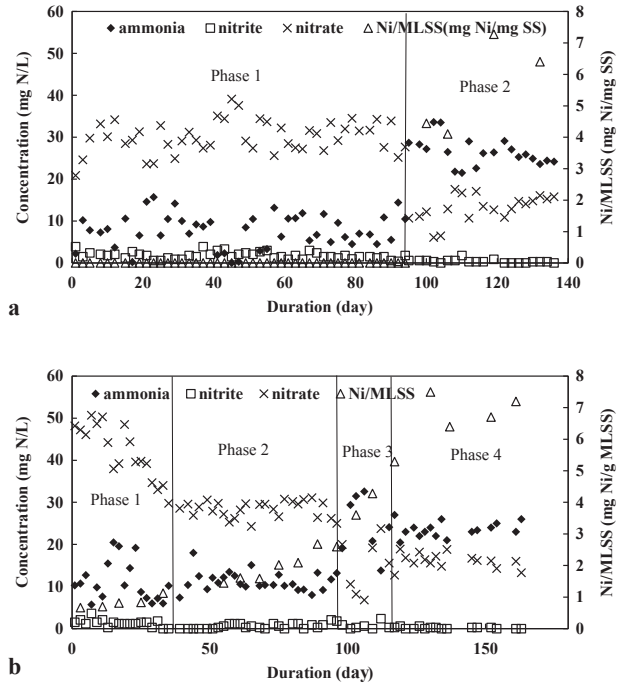

Fig. 1 – Effluent ammonia, nitrite, and nitrate concentrations and Ni/MLSS ratio of SBR 1 (a) and SBR 2 (b).

beginning of phase 2, a significant drop of AOB activity was observed between day 91 and day 104, with the worst effluent NH_4-N, NO_2-N, and NO_3-N concentrations of 33.6, 0.3, and 6.1 mg N/L, respectively, on day 104. From day 104 to 140, acclimatization of nitrifiers to nickel at Ni/MLSS ratio of 4–7 mg Ni/g MLSS was observed, with stable effluent NH_4-N, NO_2-N, and NO_3-N concentrations of 26.6 ± 3.3, 0.4 ± 0.4, and 13.0 ± 3.1 mg N/L, respectively. Compared with phase 1, the final average ACR dropped by 58% due to nickel addition.

The operation of SBR 2 can be divided into four phases based on performance, that is, phase 1 from day 0 to day 34 as start-up period, phase 2 from day 35 to day 95 as steady-state period, phase 3 from day 96 to day 112 as unstable period, and phase 4 from day 113 to day 164 as adaptation to an extremely high Ni/MLSS ratio of 5–7 mg Ni/g SS. The initial biomass could convert 40–50 mg N/L of ammonia, which is higher than that of 30–40 mg N/L in SBR1, due to higher initial RAS concentration (1.4 g/L versus 1.0 g/L). After around 1 month, relatively stable effluent with constant ammonia, nitrite, and nitrate concentrations of 11.2 ± 2.2, 0.6 ± 0.6, and 28.4 ± 1.9 mg N/L, respectively, were observed for 60 days (phase 2). The average ACR and NAR were 72.1% ± 4.9% and 2.1% ± 2.1%, respectively. Ni/MLSS ratio is one of the major parameters for nickel inhibition. During phases 1 and 2, the Ni/MLSS ratio was below 2.6 mg Ni/g MLSS, and no obvious nickel inhibition was observed. Phase 3 starting on day 98, when the Ni/MLSS reached 2.7 mg Ni/g MLSS, a significant drop of nitrifiers' activity was observed. In the following week, the performance deteriorated with effluent NH_4-N, NO_2-N, and NO_3-N concentrations of 32.6, 0.6, and 6.8 mg N/L on day 106, respectively. During phase 4 (day 112–163), the biomass acclimatized to nickel at Ni/MLSS ratio of 5–7 mg Ni/g MLSS with relatively stable effluent NH_4-N, NO_2-N, and NO_3-N concentrations of 23.0 ± 2.8, 0.3 ± 0.5, and 16.5 ± 2.4 mg N/L. Compared with SBR1 phase 1, the final average ACR dropped by 47%.

One-wayANOVA analysis suggested that the differences in effluent quality data are statistically significant at the 95% confidence limit for SBR 1 phase 1 and SBR 2 phase 2 within which the Ni/MLSS ratio in both SBRs varied from 0 to 2.7 mg Ni/g MLSS, and SBR 1 phase 2 and SBR 2 phase 4 within which the Ni/MLSS ratio in both SBRs varied from 4 to 7 mg Ni/g MLSS.

Fig. 2a and b show the mixed liquor suspended solids (MLSS), effluent suspended solids (SS), and SRTs for SBRs 1 and 2, respectively. In this study, both SBRs were operated at long SRTs. The average, maximum, and minimum SRTs of SBR 1 were 71, 83, and 56 days, respectively. The average, maximum and minimum SRTs of SBR 2 were 64, 75, and 50 days, respectively.

The initial inoculum concentrations were 1.0 g SS/L and 1.4 g SS/L for SBR 1 and SBR 2, respectively, with a volatile fraction of 77%. MLSS decreased with time for both SBRs due to the decay of heterotrophic bacteria as there was no COD in the influent, which is similar to our previous observations (Liu et al., 2017a, 2018). The MLSS concentration in SBR 1 was 280 ± 14 mg MLSS/L between day 66 and day 91 during phase 1, and 100–125 mg MLSS/L between day 120 and day 140 during phase 2. The MLSS concentration in SBR 2 was 125–140 mg/L between days 130 and 160 during phase 4. By comparing the MLSS in SBR 2 phase 4 and MLSS in SBR 1 phase 1, long-term 1 mgNi/L dose caused around 53% MLSS reduction. The effluent TSS concentration in SBR1 decreased from an initial value of 18 to 3.9 ± 0.2 mg/L on days 66–91, and decreased further to 2.1 ± 0.6 mg/L on days 100–133. Similarly, the effluent TSS concentration in SBR2 decreased from an initial value of 27 to 2.5 ± 0.4 mg/L on days 109–160.

2.2. Online batch tests

Online batch tests results are shown in Fig. 3. The Ni/MLSS ratio (Fig. 1a–1b) in SBR 2 between days 120 and 140 ranged from 5.2 to 7.5 mg Ni/g MLSS. At the ambient ammonia concentrations of 17–26 mg N/L, nitrite concentration of 0.2–0.6 mg N/L, and the pH of 7.0–7.5, the free ammonia (FA) concentration was 0.04–0.19 mg/L while free nitrous acid (FNA) was almost 0–0.007 mg/L. Anthonisen et al. (1976) reported nitrification inhibition at a FA range from 10 to 150 mg N/L for AOB and 0.1–1.0 mg N/L for NOB at 10–23°Cand pH 6–9, respectively. Neufeld et al. (1986) reported the FA inhibition threshold for AOB of 10 mg N/L at pH 8.0 and temperature of 22–40°C. Bae et al. (2001) reported that NOB activity was not inhibited at a FA concentration of less than 0.5 mg N/L, pH of 7–10, and temperature of 30°C. Wong-Chong and Loehr (1975) observed that NOB were inhibited at a FA concentrations of 3.5 mg N/L at pH 6.0–8.5 and temperature of 9–35°C. Mauret et al. (1996) found that NOB was inhibited by FA in the range of 6.6–8.9 mg N/L at pH 7–8.5 and temperature 15–25°C. In light of the above-referenced studies since the estimated concentrations of FA and FNA were respectively 0.04–0.19 and 0–0.007 mg N/L, well below the values reported above, FA and FNA inhibition was presumed not to have occurred. Alkalinity was sufficient as the influent alkalinity-to-ammonia ratio was 7.14 mg $CaCO_3$/mg NH_4-N while around 13–16 mg NO_3-N/L accumulated in the effluent.

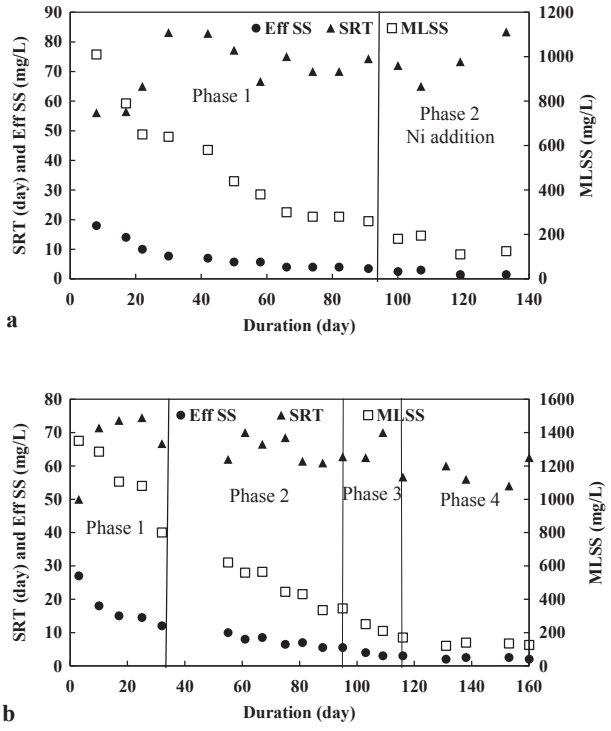

Fig. 2 – MLSS, effluent SS (Eff SS), and SRTs of SBR 1 (a) and SBR 2 (b).

Influent alkalinity was about 330 mg $CaCO_3$/L, and effluent alkalinity was around 130 to 170 mg $CaCO_3$/L, with around 160 to 200 mg $CaCO_3$/L consumed.

The AOR at DOs of 7.4, 5.0, and 3.0 mg/L were 0.79, 0.66, and 0.59 mg N/L-hr, respectively. The AOR at a DO of 5.2 mg/L was 1.7 mg N/L-hr at 14°C without nickel inhibition (Liu et al., 2018). Considering a temperature coefficient of 1.072 for AOB (Metcalf and Eddy, 2013), the estimated AOR without nickel inhibition at DO of 5.2 mg/L at 10°C is 1.3 mg N/L-hr. Thus, the AOR value of 0.66 mg N/L-hr at DO of 5.0 mg/L observed here with nickel concentration of 1 mg/L and Ni/MLSS ratio of 5.2–7.5 mg Ni/g MLSS suggests about 50% inhibition. Based on the AORs at different DOs, the estimated AOR_{max} and $K_{O,AOB}$, using Eq. 9, were 0.98 mg N/L-hr and 2.08 mg O_2/L, respectively.

Based on the starvation test, the decay coefficient (*b*) of nitrifiers was calculated as 0.098 day^{-1} at 10°C. The reported *b* value at 14°C was in the range of 0.035–0.13/day with a temperature coefficient of 1.029 (Liu et al., 2018; Metcalf and Eddy, 2013). Thus, the *b* value at 10°C is estimated to be in the range of 0.031–0.115/day, i.e., the *b* value of 0.098/day reported here is well within the range.

Thus, based on Eq. (7), using the average effluent concentrations of SBR 2 between days 112–140 (Appendix A Table SI 2), and AOR_{max} of 0.98 mg N/L-hr, the maximum growth rate of AOB ($\mu_{max,AOB}$) at 10°C was 0.16/day with nickel inhibition. The reported $\mu_{max,AOB}$ at 14°C ranges from 0.13 to 0.99/day with a median value of 0.47/day (Liu et al., 2018). The typical temperature coefficient for $\mu_{max,AOB}$ is 1.072 (Metcalf and Eddy, 2013). Thus, the estimated $\mu_{max,AOB}$ at 10°C range from 0.10 to 0.75/day. The $\mu_{max,AOB}$ value of 0.16/day falls within the aforementioned range, albeit much lower than the 0.35/day based on the median without inhibition.

2.3. *Offline batch acute toxicity tests*

The offline batch tests results at 10, 23, and 35°C are summarized below in Fig. 4. From Fig. 4, it can be seen that: (1) At 10°C, the acute nickel toxicity is predominantly to AOB, with equal or less inhibition for NOB; (2) at 23°C, the acute nickel toxicity was more serious for NOB rather than AOB; (3) at 35°C, the acute nickel toxicity was much more serious for NOB rather than AOB.

Fig. 4 also focused on the data for batches B and F operating at the same initial Ni-to-MLSS ratio but different Ni concentrations. It is evident that both batches B and F exhibited very similar SAOR and SNOR, clearly indicating that Ni toxicity is not related to Ni concentration but to Ni-to-MLSS ratio.

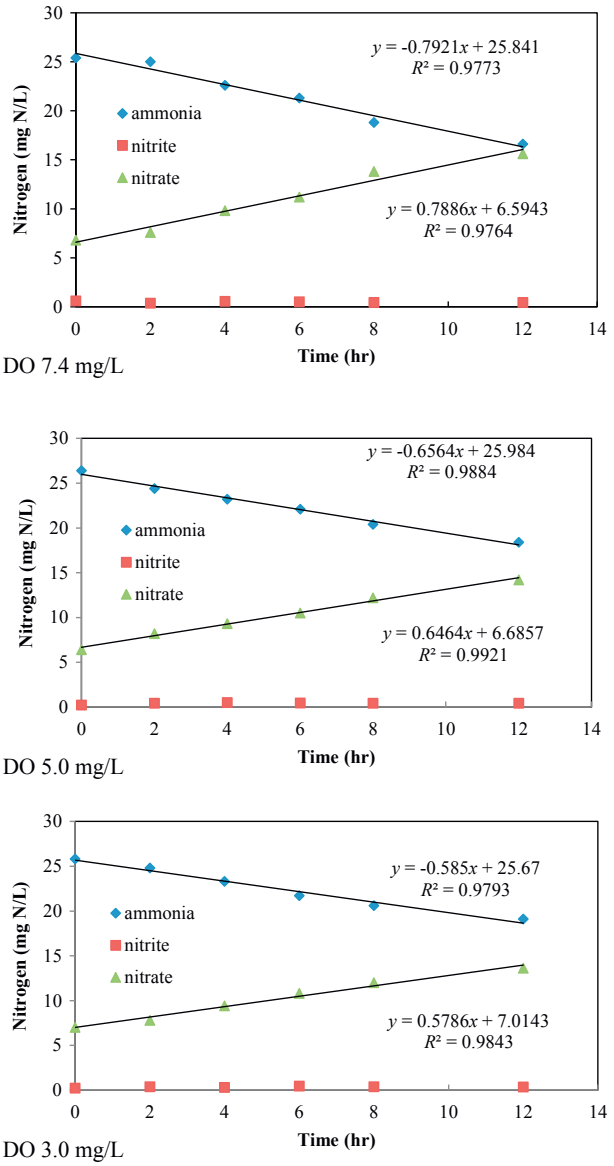

Fig. 3 – Online batch tests at different DOs in SBR 2.

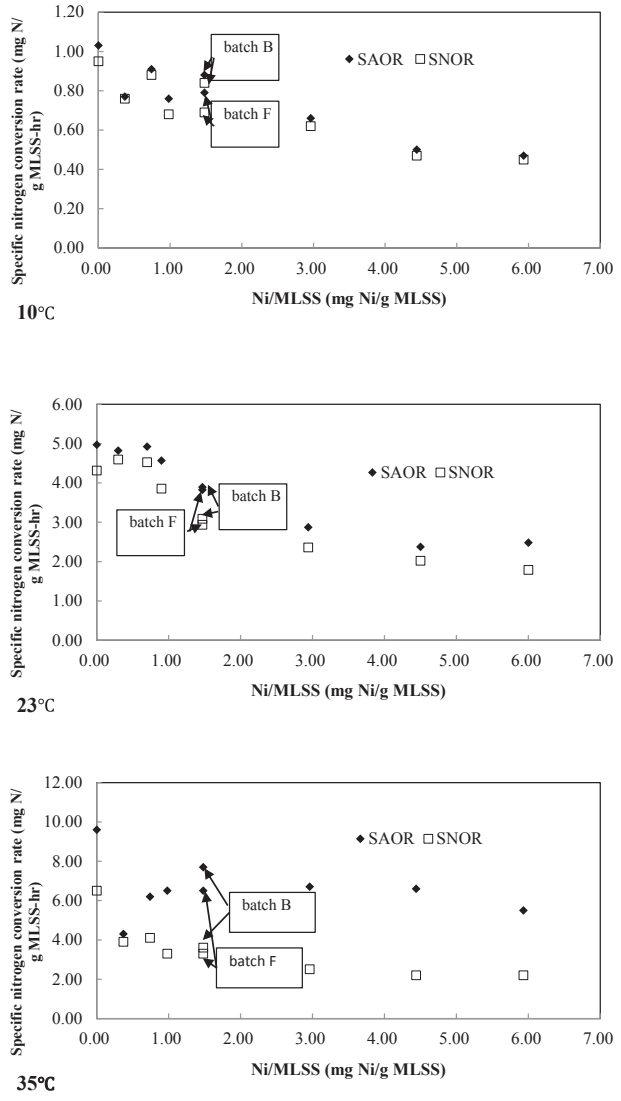

Fig. 4 – Specific ammonia oxidation rate (SAOR) and specific nitrite oxidation rate(SNOR) versus Ni/MLSS at 10, 23, and 35°C.

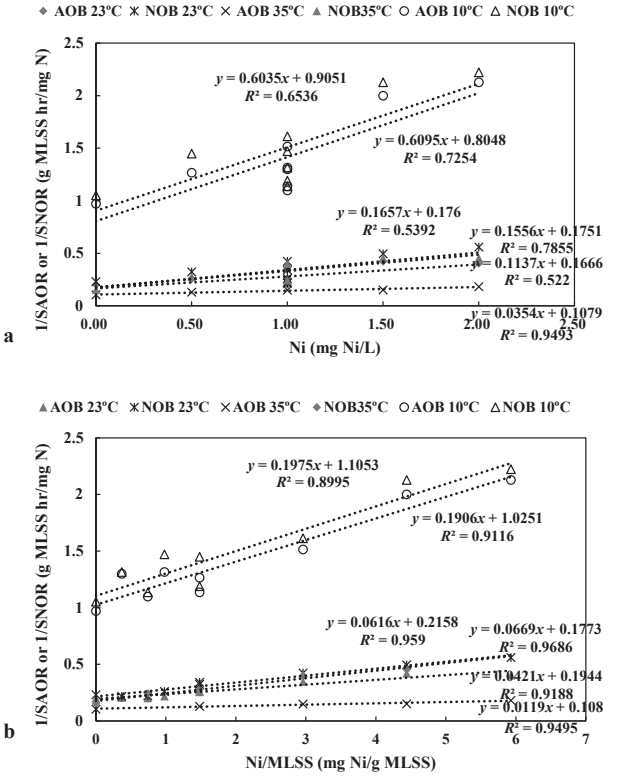

Fig. 5 – 1/SAOR and 1/SNOR versus Ni (a) and Ni/MLSS (b) at 10, 23, and 35°C.

To further describe the short-term nickel inhibition on AOB and NOB activity, non-competitive and modified non-competitive inhibition models were assessed. The half-velocity inhibition constant, which is equal to the concentration corresponding to 50% inhibition of the maximum growth rate (IC50), was determined through linearization of Eqs. (15)–(16), and (19)–(20), as illustrated in Fig. 5a and b for the non-competitive inhibition model and the modified non-competitive inhibition model, respectively. Generally, the curve based on Ni/MLSS ratio (Fig. 5b) fitted the experimental data better as evidenced by the higher R^2 values compared to Fig. 5a, suggesting that the modified non-competitive inhibition model is better than non-competitive inhibition model in terms of accuracy.

Based on Fig. 5b, the half-velocity inhibition constants based on Ni/MLSS ratio were calculated by Eqs. (19) and (20), and are presented in Table 2. Some publications reported that it is free nickel rather than total nickel that leads to inhibition (Hu et al., 2003; Sato et al., 1986). At 10, 23, and 35°C, the free nickel to total nickel ratio are 77%, 70%, and 65%, respectively. The $K_{I,Ni}$ based on free nickel to MLSS ratio at three temperatures are shown in Table 4 as well. Nickel inhibition seems more serious for AOB at 10 and 23°C than at 35°C, while the nickel inhibition for NOB increased with temperature. Based on model, it is impossible to achieve nitrite accumulation at low temperature by nickel inhibition because both AOB and NOB are equally inhibited by Ni as reflected by very close K_I values. On the contrary, there should be nitrite accumulation at 35°C with nickel inhibition, which was observed by Aslan and Sozudogru (2017).

2.4. Reversibility of acute nickel toxicity

The reversibility of acute nickel toxicity was evaluated by offline batch tests as mentioned above in Section 1.7. The results of offline batch tests are illustrated in Table 3. Based on Table 3, acute nickel toxicity to nitrifying bacteria with 2 hr contact time is reversible because the AOR and NOR in batch A (RAS without nickel) and batch B (RAS with nickel for 2 hr and washed prior to nitrification test) are very similar. On the other hand, the AOR and NOR for batch C (RAS with nickel during the batch nitrification test) were much lower than both batches A and B. The results of this study agree with the finding of Semerci and Çeçen (2007) that acute Cr inhibition of nitrification with 30 min contact time was completely reversible upon removal of Cr addition.

Table 2 – Nickel inhibition constant for AOB and NOB at 10, 23, and 35°C.

Bacteria species	Temperature (°C)	Maximum SAOR or SNOR (mg N/g MLSS-hr)	$K_{I,Ni}$ (mg Ni/g MLSS) based on total nickel concentration	$K_{I,Ni}$ (mg Ni/g MLSS) based on free nickel concentration
AOB	10	1.0	5.4	4.1
	23	5.2	4.6	3.2
	35	9.3	9.1	5.9
NOB	10	0.9	5.6	4.3
	23	4.6	3.5	2.5
	35	5.7	2.7	1.8

AOB: ammonia oxidation bacteria; NOB: nitrite oxidation bacteria; SAOR: specific ammonia oxidation rate; SNOR: specific nitrite oxidation rate; $K_{I,Ni}$: half-velocity inhibition nickel concentration.

2.5. Comparison of chronic and acute toxicity

Fig. 4 shows that at 10°C, AOB activity dropped by 9%–12% due to acute nickel toxicity at Ni/MLSS ratio below 1.5 mg Ni/g MLSS. Accordingly, during SBR 2 phase 2, AOB activity dropped by 8.3% compared with SBR 1 phase 1 at the Ni/MLSS ratio of 1.0–2.0 mg Ni/g MLSS, which agrees with the acute nickel toxicity tests. In addition, a significant drop of AOB activity (33%) was observed in acute nickel toxicity tests at Ni/MLSS ratio of 2.7 mg Ni/g MLSS. In SBR 2, on day 98, when Ni/MLSS reached 2.7 mg Ni/g MLSS, significant drop of AOB and NOB activity by 34% was observed, which corroborates the acute nickel toxicity tests results. Besides, based on Fig. 5, AOB activity dropped by 43%–57% in the acute toxicity test at 10°C at Ni/MLSS ratio of 4–7 mg Ni/g MLSS, which is in agreement with the activity loss of 47% in SBR 2, during phase 4 and 58% in SBR 1 during phase 2 (Appendix A Table SI 2). In summary, the results of the long-term SBRs operation and short-term batch tests were comparable. Based on the results of this study, the effect of acclimatization in essence reduced inhibition by about 20% (from 58% in SBR 1 phase 2 to 47% in SBR 2 phase 4).

Table 3 – Offline reversibility batch tests results.

Test No.	AOR (mg N/L-hr)	NOR (mg N/L-hr)
A	1.7	1.5
B	1.6	1.4
C	1.0	0.8

AOR: ammonia oxidation rate; NOR: nitrite oxidation rate.

2.6. Comparison with literature

This study demonstrated that nickel inhibition is affected by Ni/MLSS ratio rather than nickel concentration, which is consistent with the observations of Randall and Buth (1984), and Sujarittanonta and Sherrard (1981). On the contrary, recently, Hernandez-Martinez et al. (2018) studied nickel inhibition of activated sludge and reported that nickel inhibition is independent of biomass concentration. However, a very high nickel concentration of 40 mg/L which resulted in a Ni/MLSS ratio of 13–100 mg Ni/g SS was adopted. At this high Ni/MLSS ratio range, based on the modified model in this study, the nickel inhibition of AOB varied from 74% to 95%.

At 35°C, Aslan and Sozudogru (2017) ran a submerged biofilter (SBFR) and observed nitrite accumulation as total

Table 4 – IC50 values for nickel inhibition.

IC50 for AOB (mg Ni/L)	IC50 for NOB (mg Ni/L)	IC50 for AOB based on Ni/MLSS (mg Ni/g SS)	IC50 for NOB based on Ni/MLSS (mg Ni/g SS)	Temperature (°C)	Reference
5.0–5.8		9.0–10.5		26	Çeçen et al. (2010)
2.59–3.02		4.7–5.5			Çeçen et al. (2010) based on free nickel
2.0–5.0		1.3–2.4		room	You et al. (2009)
58.5				26	Hu et al. (2004)
33				20	Insel et al. (2006)
>4	4			35	Aslan and Sozudogru (2017)
0.7*	0.7	0.2*	0.5	14	Randall and Buth (1984)
		0.3–0.4		21	Sujarittanonta and Sherrard (1981)
1.9		5-6		25	Kapoor et al. (2015)
10.8–16.2	11.2–16.8	5.4	5.6	10	This study
10.4–15.6	9.2–13.8	4.6	3.5	23	
18.2–27.3	5.4–8.1	9.1	2.7	35	
8.2–12.3	8.6–12.9	4.1	4.3	10	This study based on free nickel
6.4–9.6	5.0–7.5	3.2	2.5	23	
11.8–17.7	3.6–5.4	5.9	1.8	35	

IC50: half maximal inhibitory concentration.
* IC30 calculated based on long-term performance.

nickel increased from 0 to 4 mg/L. On the contrary, Randall and Buth (1984) reported that no nitrite accumulation was observed at total nickel dose of 2.8 mg/L, which corresponded to 1.9 mg Ni/g MLSS at 35°C. Based on the results of this work, nitrite accumulation should be achieved at 35°C.

The IC50 based on total nickel concentration from the literature are compared with this study and shown in Table 4 (Aslan and Sozudogru, 2017; Çeçen et al., 2010; Hu et al., 2004; Insel et al., 2006; Kapoor et al., 2015; Randall and Buth, 1984; Sujarittanonta and Sherrard, 1981; You et al., 2009). Considering the typical MLSS concentration in waste activated sludge of 2–3 g/L, the IC50 values at 10, 23, and 35°C were calculated by multiplying the $K_{I,Ni}$ and the typical MLSS concentration. As evident from Table 4, the range of IC50 values for AOBs from the literature is very wide. In addition, there is very limited information on the IC50 values for NOB. The IC50 value for NOB calculated based on effluent ammonia, nitrite and nitrate concentration in the long-term study of Randall and Buth (1984) was 0.7 mg Ni/L, which corresponded to 0.5 mg Ni/g SS at 14°C. Kapoor et al. (2015) conducted the nickel toxicity batch tests on nitrification at 25°C and reported the IC50 value of 1.9 mg/L for AOB, which corresponds to 5–6 mg Ni/g SS, close to the 4.6 mg Ni/g SS reported for AOB at 23°C in this study.

3. Conclusions

This paper is the first study that conducted short-term batch tests based on nickel concentration and biomass concentration at three different temperatures and our results suggested that: (1) it is the Ni/MLSS ratio rather than nickel concentration that governs toxicity; (2) both sludge type i.e., RAS and nitrfiers, and the exposure mode are not crucial, as evidenced by similar acute and chronic nickel inhibition extent in SBRs operation and batch tests at similar Ni/MLSS ratios; (3) the nickel toxicity to nitrifiers is significantly affected by temperature, as evidenced by AOB IC50 of 5.4, 4.6, and 9.1 mg Ni/g SS and NOB IC50 of 5.6, 3.5, and 2.7 mg Ni/g SS at 10, 23, and 35°C. At 10°C, the acute nickel toxicity is predominantly to AOB, with equal or less inhibition for NOB. At 23°C, the acute nickel toxicity was more serious for NOB rather than AOB; at 35°C, the acute nickel toxicity was much more serious for NOB rather than AOB.

Chronic and acute inhibition results with respect to the extent of inhibition and corresponding Ni/MLSS ratio were consistent. AOB activity dropped by 47% in SBR 2 phase 4 and 58% in SBR1 phase 2 at Ni/MLSS ratio of 4–7 mg Ni/g MLSS, indicating that after long-term acclimatization, nitrifiers are more tolerant to nickel inhibition at 10°C. Short-term nickel inhibition of nitrifying bacteria was reversible.

Based on this study, it is impossible to achieve partial nitrification at 10°C by nickel dose. On the contrary, combination of nickel addition and SRT control could be a possible way to realize partial nitrification at 35°C.

Conflicts of interest

There are no conflicts of interest to declare.

Acknowledgments

This work was supported by the Natural Sciences and Engineering Research Council of Canada (No. CRDPJ 458990-13).

Appendix A. Supplementary data

Supplementary data to this article can be found online at https://doi.org/10.1016/j.jes.2019.03.009.

REFERENCES

Akhtar, M.F., Ashraf, M., Javeed, A., Anjum, A.A., Sharif, A., Saleem, M., et al., 2018. Association of textile industry effluent with mutagenicity and its toxic health implications upon acute and sub-chronic exposure. Environ. Monit. Assess. 190, 179.

Anthonisen, A.C., Loehr, R.C., Prakasam, T.B.S., Srinath, E.G., 1976. Inhibition of nitrification by ammonia and nitrous acid. J. Water Pollut. Control Fed. 835–852.

APHA, 2005. Standard Methods for the Examination of Water & Wastewater. American Public Health Association/American Water Works Association/Water Environment Federation, Washington DC.

Aslan, S., Sozudogru, O., 2017. Individual and combined effects of nickel and copper on nitrification organisms. Ecol. Eng. 99, 126–133.

Bae, W., Baek, S., Chung, J., Lee, Y., 2001. Optimal operational factors for nitrite accumulation in batch reactors. Biodegradation. 12, 359–366.

Blum, D.J.W., Speece, R., 1991. A database of chemical toxicity to environmental bacteria and its use in interspecies comparisons and correlations. J. Water Pollut. Control Fed. 63, 198–207.

Buch, A.C., Niemeyer, J.C., Correia, M.E.F., Silva-Filho, E.V., 2016. Ecotoxicity of mercury to *Folsomia candida* and *Proisotoma minuta* (Collembola: Isotomidae) in tropical soils: baseline for ecological risk assessment. Ecotoxicol. Environ. Saf. 127, 22–29.

Carletti, G., Fatone, F., Bolzonella, D., Cecchi, F., Carletti, G., 2008. Occurrence and fate of heavy metals in large wastewater treatment plants treating municipal and industrial wastewaters. Water Sci. Technol. 57, 1329–1336.

Çeçen, F., Semerci, N., Geyik, A.G., 2010. Inhibitory effects of Cu, Zn, Ni and Co on nitrification and relevance of speciation. J. Chem. Technol. Biotechnol. 85, 520–528.

Cheng, L., Li, X., Jiang, R., Wang, C., Yin, H.B., 2011. Effects of Cr(VI) on the performance and kinetics of the activated sludge process. Bioresour. Technol. 102, 797–804.

Chipasa, K.B., 2003. Accumulation and fate of selected heavy metals in a biological wastewater treatment system. Waste Manag. 23, 135–143.

Communities, E., 2001. Pollutants in urban wastewater and sewage sludge. Office for Official Publications of the European Communities, Luxembourg.

Dilek, F.B., Gökçay, C.F., 1996. Microbiology of activated sludge treating wastewater containing Ni(II) and Cr(VI). Water Sci. Technol. 34, 183–191.

Gadd, G.M., Griffiths, A.J., 1977. Microorganisms and heavy metal toxicity. Microb. Ecol. 4, 303–317.

Ge, S., Wang, S., Yang, X., Qiu, S., Li, B., Peng, Y., 2015. Detection of nitrifiers and evaluation of partial nitrification for wastewater treatment: a review. Chemosphere. 140, 85–98.

Gikas, P., 2008. Single and combined effects of nickel (Ni(II)) and cobalt (Co(II)) ions on activated sludge and on other aerobic microorganisms: a review. J. Hazard. Mater. 159, 187–203.
Gustafsson, J.P., 2013. Visual MINTEQ Version 3.1. Department of Sustainable Development. Environmental Science and Engineering, KTH, Stockholm.
Hellinga, C., Schellen, A., Mulder, J.W., van Loosdrecht, M., Heijnen, J.J., 1998. The SHARON process: an innovative method for nitrogen removal from ammonium-rich waste water. Water Sci. Technol. 37, 135–142.
Hernandez-Martinez, G.R., Ortiz-Alvarez, D., Perez-Roa, M., Urbina-Suarez, N.A., Thalasso, F., 2018. Multiparameter analysis of activated sludge inhibition by nickel, cadmium, and cobalt. J. Hazard. Mater. 351, 63–70.
Hu, Z., Chandran, K., Grasso, D., Smets, B.F., 2003. Impact of metal sorption and internalization on nitrification inhibition. Environ. Sci. Technol. 37, 728–734.
Hu, Z., Chandran, K., Grasso, D., Smets, B.F., 2004. Comparison of nitrification inhibition by metals in batch and continuous flow reactors. Water Res. 38, 3949–3959.
Insel, G., Karahan, O., Ozdemir, S., Pala, L., Katipoglu, T., Cokgor, E. U., et al., 2006. Unified basis for the respirometric evaluation of inhibition for activated sludge. J. Environ. Sci. Health A Tox. Hazard. Subst. Environ. Eng. 41, 1763–1780.
Kapoor, V., Li, X., Elk, M., Chandran, K., Impellitteri, C.A., Santo Domingo, J.W., 2015. Impact of heavy metals on transcriptional and physiological activity of nitrifying bacteria. Environ. Sci. Technol. 49, 13454–13462.
Karvelas, M., Katsoyiannis, A., Samara, C., 2003. Occurrence and fate of heavy metals in the wastewater treatment process. Chemosphere. 53, 1201–1210.
Keithly, J., Brooker, J.A., Deforest, D.K., Wu, B.K., Brix, K.V., 2004. Acute and chronic toxicity of nickel to a cladoceran (*Ceriodaphnia dubia*) and an amphipod (*Hyalella azteca*). Environ. Toxicol. Chem. 23, 691–696.
Leonard, E.M., Barcarolli, I., Silva, K.R., Wasielesky, W., Wood, C. M., Bianchini, A.J., et al., 2011. The effects of salinity on acute and chronic nickel toxicity and bioaccumulation in two euryhaline crustaceans: *Litopenaeus vannamei* and *Excirolana armata*. Comp. Biochem. Physiol. C Toxicol. Pharmacol. 154, 409–419.
Lewandowski, Z., 1987. Behaviour of biological reactors in the presence of toxic compounds. Water Res. 21, 147–153.
Li, X., Kapoor, V., Impelliteri, C., Chandran, K., Domingo, J.W.S., 2016. Measuring nitrification inhibition by metals in wastewater treatment systems: current state of science and fundamental research needs. Crit. Rev. Environ. Sci. Technol. 46, 249–289.
Liu, G., Wang, J., 2014. Role of solids retention time on complete nitrification: mechanistic understanding and modeling. J. Environ. Eng-ASCE. 140, 48–56.
Liu, X., Kim, M., Nakhla, G., 2017a. Operational conditions for successful partial nitrification in a sequencing batch reactor (SBR) based on process kinetics. Environ. Technol. 38, 694–704.
Liu, X., Kim, M., Nakhla, G., 2017b. A model for determination of operational conditions for successful shortcut nitrification. Environ. Sci. Pollut. R. 24, 3539–3549.
Liu, X., Kim, M., Nakhla, G., 2018. Performance and kinetics of nitrification of low ammonia wastewater at low temperature. Water Environ. Res. 90, 498–509.
Mauret, M., Paul, E., Puech-Costes, E., Maurette, M., Baptiste, P., 1996. Application of experimental research methodology to the study of nitrification in mixed culture. Water Sci. Technol. 34, 245–252.
Metcalf, Eddy, 2013. Wastewater Engineering: Treatment and Reuse. McGraw-Hill Education.
Neufeld, R., Greenfield, J., Rieder, B., 1986. Temperature, cyanide and phenolic nitrification inhibition. Water Res. 20, 633–642.
Nies, D.H., 1999. Microbial heavy metal resistance. Appl. Microbiol. Biotechnol. 51, 730–750.
Pereira, C.M., Deruytter, D., Blust, R., De Schamphelaere, K.A.C., 2017. Effect of temperature on chronic toxicity of copper, zinc, and nickel to *Daphnia magna*. Environ. Toxicol. Chem. 36, 1909–1916.
Randall, C., Buth, D., 1984. Nitrite build-up in activated sludge resulting from combined temperature and toxicity effects. J. Water Pollut. Control Fed. 56, 1045–1049.
Sato, C., Schnoor, J.L., McDonald, D.B., 1986. Effects of copper and nickel on the growth of Nitrosomonas europaea. Environ. Toxicol. Water Qual. 1, 357–376.
Semerci, N., Çeçen, F., 2007. Importance of cadmium speciation in nitrification inhibition. J. Hazard. Mater. 147, 503–512.
Soliman, M., Eldyasti, A., 2018. Ammonia-oxidizing bacteria (AOB): opportunities and applications—a review. Rev. Environ. Sci. Biotechnol. 17, 285–321.
Stasinakis, A.S., Mamais, D., Thomaidis, N.S., Lekkas, T.D., 2002. Effect of chromium (VI) on bacterial kinetics of heterotrophic biomass of activated sludge. Water Res. 36, 3341–3349.
Sujarittanonta, S., Sherrard, J.H., 1981. Activated sludge nickel toxicity studies. J. Water Pollut. Control Fed. 53, 1314–1322.
Sun, J., Yang, Q., Wang, D., Wang, S., Chen, F., Zhong, Y., et al., 2017. Nickel toxicity to the performance and microbial community of enhanced biological phosphorus removal system. Chem. Eng. J. 313, 415–423.
Teijon, G., Candela, L., Tamoh, K., Molina-Díaz, A., Fernández-Alba, A.R., 2010. Occurrence of emerging contaminants, priority substances (2008/105/CE) and heavy metals in treated wastewater and groundwater at Depurbaix facility (Barcelona, Spain). Sci. Total Environ. 408, 3584–3595.
Wong-Chong, G., Loehr, R., 1975. The kinetics of microbial nitrification. Water Res. 9, 1099–1106.
Yang, Q., Sun, J., Wang, D., Wang, S., Chen, F., Yao, F., et al., 2017. Effect of nickel on the flocculability, settleability, and dewaterability of activated sludge. Bioresour. Technol. 224, 188–196.
Yeung, C.H., Francis, C.A., Criddle, C.S., 2013. Adaptation of nitrifying microbial biomass to nickel in batch incubations. Appl. Microbiol. Biotechnol. 97, 847–857.
Yin, K., Lv, M., Wang, Q., Wu, Y., Liao, C., Zhang, W., et al., 2016. Simultaneous bioremediation and biodetection of mercury ion through surface display of carboxylesterase E2 from *Pseudomonas aeruginosa* PA1. Water Res. 103, 383–390.
You, S.J., Tsai, Y.P., Huang, R.Y., 2009. Effect of heavy metals on nitrification performance in different activated sludge processes. J. Hazard. Mater. 165, 987–994.
Yuan, L., Zhi, W., Liu, Y., Karyala, S., Vikesland, P., Chen, X., et al., 2014. Lead toxicity to the performance, viability, and community composition of activated sludge microorganisms. Environ. Sci. Technol. 49, 824–830.
Zhu, G., Peng, Y., Li, B., Guo, J., Yang, Q., Wang, S., 2008. Biological Removal of Nitrogen from Wastewater, Rev. Environ. Contam. Toxicol. Springer, New York, pp. 159–195.